Theory of a compound large-angle atom beam splitter

A. Zh. Muradyan and A. A. Poghosyan
Department of Physics, Yerevan State University, 1 Alex Manookian, Yerevan 375025, Armenia

P. R. Berman
Michigan Center for Theoretical Physics, FOCUS Center, and Department of Physics, University of Michigan, Ann Arbor, Michigan 48109-1012, USA

(Received 18 February 2003; published 12 September 2003)

A theory of an atom beam splitter is developed involving the interaction of standing-wave field pulses with Λ-type atoms. The beam splitter consists of *two* interaction zones, both treated in the Raman-Nath approximation. There is an initial, off-resonant field (or fields) that prepares the initial atomic state, followed by interaction with a pair of standing-wave field pulses. Using this configuration one is able to create a large-angle beam splitter with a significant suppression of unwanted momentum components. The roles of relaxation and a frequency chirp are investigated, as are initial conditions for which both ground states of the Λ scheme are prepared by the first field. It is shown that the scheme is rather robust against fluctuations of system parameters.

DOI: 10.1103/PhysRevA.68.033604 PACS number(s): 03.75.Be

I. INTRODUCTION

Atom interferometers [1] often rely on the manipulation of the translational motion of atoms by coherent laser radiation. The underlying physical mechanism responsible for the deflection of atoms by fields is the momentum exchange between the atoms and the fields. In each act of absorption or emission the atom acquires or loses a quantum of momentum $\hbar\mathbf{k}$, where $\mathbf{k}$ is the radiation field wave vector. Atom interferometers require, as a rule, that the atomic wave packet is split and then recombined, in analogy with optical interferometers. In reality, owing to the internal structure of atoms, the picture of interference for atomic wave packets is more complex than for the light waves. In particular, it is possible to construct interferometers that rely on interference between atomic internal states (internal state atom interferometry) rather than on interference between center-of-mass momentum states (matter-wave interferometry). In this paper we do not focus on atom interferometry *per se*, but instead look at the momentum distribution produced in a matter-wave beam splitter. One of the major challenges in atom interferometry is the generation of sufficiently large momentum splitting. Owing to the relatively large values of atomic masses, the splitting angle is very small for one-photon exchange process between the radiation field and an atom. Several schemes for achieving large-angle atom beam splitters have been proposed. For instance, in Ref. [2], a series of counterpropagating laser pulses was used to increase the separation between atoms in different magnetic substates that were prepared in different arms of an atom interferometer. A related method, robust with respect to the values of field strengths required, involves the adiabatic transfer of population between magnetic ground state sublevels using counterpropagating laser pulses [3]. Adiabatic transfer was also proposed as a method for obtaining large-angle beam splitting in a scheme involving three-level atoms driven by a standing-wave and traveling-wave field in a STIRAP geometry [4] and then subjected to an additional standing-wave field [5]. A method for suppressing low-order diffraction using detuned fields was described in Ref. [6]. Large-angle beam splitters can also be produced using strong standing-wave fields [7], bichromatic fields [8], or magneto-optical potentials [9].

Broadly speaking, atom beam splitters can operate in either the Bragg or the Raman-Nath regime. In the Bragg regime the interaction time is much longer than the inverse recoil frequency associated with absorption or emission, while in the Raman-Nath regime the interaction time is much less than the inverse recoil frequency. The discussion in this paper is restricted to the Raman-Nath regime. Atoms are coherently scattered by an intense standing-wave light field, resulting in Kapitza-Dirac scattering [10]. For off-resonant fields, Kapitza-Dirac scattering can result in a comb of momentum components separated by intervals of $2\hbar\mathbf{k}$ along the standing-wave direction that results from absorption (stimulated) emission processes between the counterpropagating traveling waves forming the standing-wave field.

Kapitza-Dirac scattering creates a multiple-peaked diffraction pattern, symmetrically distributed about the initial value of momentum. The distance between the two largest peaks in the distribution is approximately equal to twice the product of the Rabi frequency and the time of interaction. By ramping up the product of field intensity and interaction time (but respecting the Raman-Nath condition) one can create peak splittings as large as $10^3\hbar\mathbf{k}$ with readily available laser sources. The problem with Kapitza-Dirac scattering is that the amplitudes of the peaks intermediate between the extreme peaks are non-negligible; in other words, a standing-wave field does not act as an extremely clean beam splitter. If one could reduce or eliminate these intermediate peaks, the resulting pattern would more closely resemble that of an ideal beam splitter. Beam splitters based on bichromatic fields and magneto-optical potentials achieve this suppression with varying degrees of success [8,9].

In this paper we present and analyze another method for suppressing the intermediate peaks. Our beam splitter consists of *two* stages, both of which are based on resonant Kapitza-Dirac diffraction. As such, our beam splitter can be viewed as a *compound*, Kapitza-Dirac beam splitter. In a

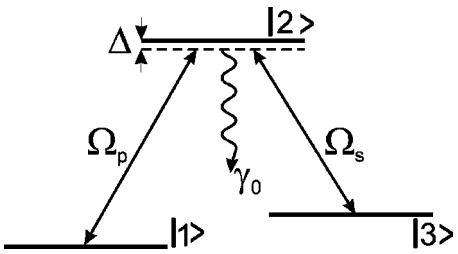

FIG. 1. Atom-field geometry: standing-wave field pulses $\Omega_p(z,t)$ and $\Omega_s(z,t)$ drive coupled atomic transitions in a Λ scheme involving states $|1\rangle$, $|2\rangle$, and $|3\rangle$. Relaxation from state $|2\rangle$ is out of the Λ system.

certain sense it is the three-level counterpart of the two-level scheme analyzed in Ref. [11]. Our scheme has the additional advantage that the same laser standing-wave pulses can be used for both stages of the beam splitter. The combined action of both stages results in a dramatic reduction in the amplitudes of the intermediate peaks, producing a much cleaner large-angle beam splitter. The role played by spontaneous decay and chirping of the applied field frequencies is also explored.

The paper is organized as follows. In Sec. II, the atom-field configuration, consisting of three-level atoms in a Λ configuration interacting with standing-wave field laser pulses, is presented. Equations are derived for the atomic momentum state amplitudes that are solved analytically for a specific choice of pulse shapes and time-dependent detunings. In Sec. III we give a brief general analysis of the momentum distribution associated with each internal atomic energy level and then make the detailed analytical and numerical study of the distribution, assuming the atoms reside initially in only one of the ground-state levels. Section IV explores the possibility of using two initially populated atomic levels to create the desired narrow distributions. In Sec. V we summarize the results.

II. MODEL AND ANALYTICAL SOLUTION

A collimated, monoenergetic atomic beam passes through two closely spaced field interaction zones. The atomic beam is oriented perpendicular to the fields' propagation vectors. The first atom-field interaction produces an initial transverse momentum distribution for the atoms; for example, if the first field is an off-resonant standing-wave field, it will produce the Kapitza-Dirac momentum distribution associated with scattering by a standing-wave field. Following this initial interaction, the atoms are subjected to a second atom-field interaction that modifies the momentum distribution created by the first field(s). The goal is to choose the fields in such a manner that, following the second interaction, the momentum distribution is dominated by two, well-separated momentum peaks. In this section, we consider the second interaction, assuming that the initial state has been prepared. The atom level scheme is the Λ or Raman scheme shown in Fig. 1. A field E_p drives the 1-2 transition and a field E_s drives the 2-3 transition. States 1 and 3 are assumed to be metastable, while state 2 decays at rate γ_0 to levels *outside* the 3-level manifold. This simplified decay scheme allows for analytical solutions using an amplitude basis. We often are interested in the limiting case where decay during the interaction is negligible. Nevertheless, if there is some residual population in the excited state after the interaction it would decay back to levels 1 and 3 and degrade the momentum distribution of those states. In our model, we allow for decay during and following the interaction, but neglect the repopulation of levels 1 and 3.

The time-dependent equations for the probability amplitudes C_1, C_2, and C_3, in the rotating wave approximation and in a frame rotating at the optical frequency, are given by

$$i\frac{\partial}{\partial t}\begin{bmatrix} C_1 \\ C_2 \\ C_3 \end{bmatrix} = \begin{bmatrix} 0 & \Omega_p(z,t) & 0 \\ \Omega_p(z,t) & \Delta - i\gamma_0 & \Omega_s(z,t) \\ 0 & \Omega_s(z,t) & 0 \end{bmatrix}\begin{bmatrix} C_1 \\ C_2 \\ C_3 \end{bmatrix}, \quad (1)$$

where $\Omega_j(z,t) = -d_j E_j(z,t)/2\hbar (j=p,s)$ are the Rabi frequencies associated with the optical transitions, d_j are dipole moment matrix elements, $E_j(z,t)$ are the electric-field amplitudes of the laser pulses, z is an atomic center-of-mass coordinate, and γ_0 is the relaxation rate. The atom-field detunings $\Delta_p = \omega_p - \omega_{21}$ and $\Delta_s = \omega_p - \omega_{23}$ are taken to be equal, $\Delta_p = \Delta_s = \Delta$ (exact two-photon resonance). The frequencies Ω_j are taken as real, since we will be concerned mainly with cases where $E_j(z,t) \sim \sin(kz)$ or $\cos(kz)$.

In the Raman-Nath approximation, the atoms are effectively frozen in the transverse direction during their interaction with the fields and the motion of the atoms parallel to the field propagation vectors can be neglected. In this limit, Eq. (1) can be solved as if the atoms were stationary with regard to their transverse motion. On the other hand, the longitudinal motion is treated classically. The calculation is carried out in a frame moving at the longitudinal atomic velocity; in this frame, atoms experience a pulse having duration T.

We will assume the same time envelope for both laser pulses,

$$\Omega_p(z,t) = \Omega_p(z) f(t), \quad \Omega_s(z,t) = \Omega_s(z) f(t), \quad (2)$$

with

$$f(t) = \mathrm{sech}(t/T). \quad (3)$$

Moreover, to allow for analytical solutions [12], we take the detuning as

$$\Delta(t) = \sigma \tanh(t/T) + \Delta_0, \quad (4)$$

where σ can be viewed as a chirp rate. Then, in full analogy with Ref. [12], we arrive at the following expressions for the lower-level atomic state amplitudes after interaction with the laser pulses ($t \to +\infty$):

$$C_1(z,+\infty) = [B\sin^2\theta + \cos^2\theta] C_1(z,-\infty) + (B-1)\sin\theta\cos\theta C_3(z,-\infty), \quad (5a)$$

$$C_3(z,+\infty)=(B-1)\sin\theta\cos\theta C_1(z,-\infty)+[B\cos^2\theta+\sin^2\theta]C_3(z,-\infty). \quad (5b)$$

Here

$$\sin\theta=\Omega_p(z)/\sqrt{\Omega_p^2(z)+\Omega_s^2(z)},$$

$$\cos\theta=\Omega_s(z)/\sqrt{\Omega_p^2(z)+\Omega_s^2(z)}, \quad (6)$$

$$B=\frac{\Gamma\left(\frac{1}{2}+\gamma+i(\delta-\beta)\right)\Gamma\left(\frac{1}{2}+\gamma+i(\delta+\beta)\right)}{\Gamma\left(\frac{1}{2}+\gamma+i\delta-\sqrt{\alpha^2(z)-\beta^2}\right)\Gamma\left(\frac{1}{2}+\gamma+i\delta+\sqrt{\alpha^2(z)-\beta^2}\right)}, \quad (7)$$

$\Gamma(x)$ is the gamma function,

$$\alpha(z)=\sqrt{\Omega_p^2(z)+\Omega_s^2(z)}T \quad (8)$$

is a dimensionless pulse area, and

$$\delta=\frac{1}{2}\Delta T, \quad \beta=\frac{1}{2}\sigma T, \quad \gamma=\frac{1}{2}\gamma_0 T, \quad (9)$$

are dimensionless central detuning, chirp rate, and decay parameters, respectively.

Since we are interested in the form of momentum distribution after the interaction, we expand the functions (5a) and (5b) in a Fourier series:

$$C_j(z,+\infty)=\sum_{n=-\infty}^{\infty}C_{j,n}(\infty)e^{2inkz},$$

with

$$C_{j,n}(\infty)=\frac{1}{2\pi}\int_0^{2\pi}C_j(z,+\infty)e^{-2inkz}d(kz), \quad (10)$$

where $j=1,3$. The coefficient C_{jn} gives the probability amplitude for the atom simultaneously to have momentum $2n\hbar k$ and be in internal state j. In writing these Fourier series, it is assumed that the *initial*-state amplitudes $C_j(z,-\infty)$ can be decomposed into a Fourier series of the form $C_j(z,-\infty)=\Sigma_{n=-\infty}^{\infty}C_{j,n}(-\infty)e^{2inkz}$ in which only even powers of $(\mathbf{k}z)$ appear.

The final-state momentum components depend on the spatial dependence of the fields and the initial values of the state amplitudes in a complicated manner. While numerical calculations are certainly possible, it is interesting first to consider special cases for which analytical solutions can be obtained. The manner in which one can construct a beam splitter based on these techniques is illustrated by these simple examples.

III. ATOMS INITIALLY IN STATE 1

In this section, it is assumed that the atoms are optically pumped into level 1 and then subjected to an off-resonant standing-wave field. As a result the atoms are prepared in an initial state having amplitudes

$$C_2(z,-\infty)=0, \quad C_3(z,-\infty)=0, \quad (11)$$

$$C_1(z,-\infty)=e^{iU\cos 2kz}=\sum_m i^m J_m(U)e^{2imkz},$$

where U is the pulse area of the preparatory field and $J_m(U)$ is a Bessel function of order m. These are the initial values to be used in Eqs. (5). We consider two special cases that allow for relatively simple solutions. Although we use the formal solutions developed in the preceding section, it should be noted that Eq. (1) can be solved directly for these special cases.

A. sin-cos or cos-sin case

When the standing-wave fields are spatially shifted by $\pi/2$ relative to one another and have the same amplitudes [13],

$$\Omega_p(z)=\Omega_p\sin kz, \quad \Omega_s(z)=\Omega_s\cos kz, \quad (12)$$

one has $\alpha=\Omega T=$ const, and B is z independent. In addition,

$$\sin\theta=\sin kz, \quad \cos\theta=\cos kz. \quad (13)$$

Since $\sin\theta\cos\theta=\sin kz\cos kz=(1/4i)(e^{i2kz}-e^{-i2kz})$, it follows from Eqs. (5b) and (10) that the momentum state amplitudes for the initially empty ground-state level 3 are given by

$$C_{3,n}(\infty)=\frac{B(\alpha,\beta,\gamma)-1}{4i}[C_{1,n-1}(-\infty)-C_{1,n+1}(-\infty)]. \quad (14)$$

Further substitution of $C_{1,m}(-\infty)=i^m J_m(U)$ from Eq. (11) yields

$$C_{3,n}(\infty)=\frac{-B(\alpha,\beta,\gamma)+1}{4}i^n[J_{n+1}(U)+J_{n-1}(U)]. \quad (15)$$

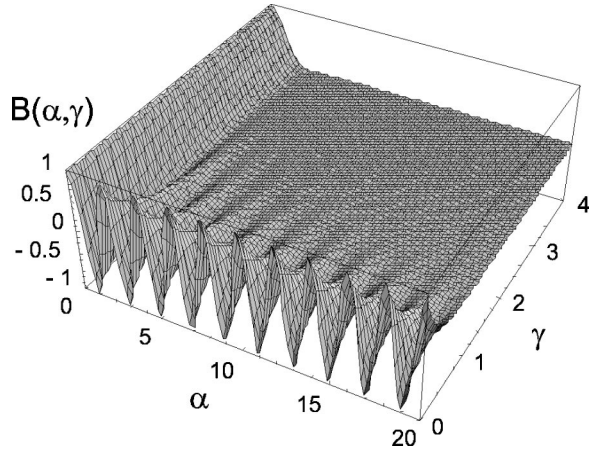

FIG. 2. Parameter B as a function of field intensity $\alpha=\Omega T$ and relaxation rate γ when $\Omega_p(z)=\Omega\cos kz$, $\Omega_s(z)=\Omega\sin kz$ (or vice versa).

Since we are interested in large momentum transfer, we choose $U\gg 1$. Then for intermediate momentum states with $|m|<U$ one may estimate the Bessel functions by [14]

$$J_m(U)\approx\sqrt{\frac{2}{\pi U}}\cos\left(U-\frac{m\pi}{2}-\frac{\pi}{4}\right), \tag{16}$$

implying that, for such states, $J_{n+1}(U)=-J_{n-1}(U)$ with high accuracy. Since $J_{n+1}(U)\approx -J_{n-1}(U)$ for these intermediate momentum states, it follows from Eq. (15) that these intermediate state amplitudes are almost completely suppressed. The final-state-3 momentum distribution, shown in Fig. 4(a) below, clearly exhibits this suppression. As a result, we achieved the desired goal. Moreover, the beam splitter acts in the manifold of a single level (level 3) and can be used in a matter-wave atom interferometer. The final-state Fourier components for state 1 vary as $[J_{n+1}(U)-J_{n-1}(U)]$ and there is no suppression of intermediate peaks. In a given experiment, one may need to remove atoms left in state 1 from the beam by some selective excitation process.

An important advantage of this scheme is that it is relatively insensitive to parameters such as field intensity, detuning and relaxation rates. What is necessary is to have equal Rabi frequencies on the coupled transitions, a $\pi/2$ spatial phase shift between the standing-wave fields, and optical pumping to a single initial state. We will see that it is possible to reduce the sensitivity of the results to the spatial phase shift.

According to Eq. (15), population transfer is optimal if $B=-1$. In order to examine what values are possible for B, let us take $\beta=0$ (no chirp), $\gamma=0$ (no relaxation). From Eq. (7) one finds

$$B(\alpha,0,0)=\cos(\pi\alpha). \tag{17}$$

The transfer efficiency is an oscillatory function of field strength, reaching a maximum for a π pulse.

To examine the role of relaxation, we take the case $\beta=\delta=0$ (exact resonance) and plot B as a function of α and

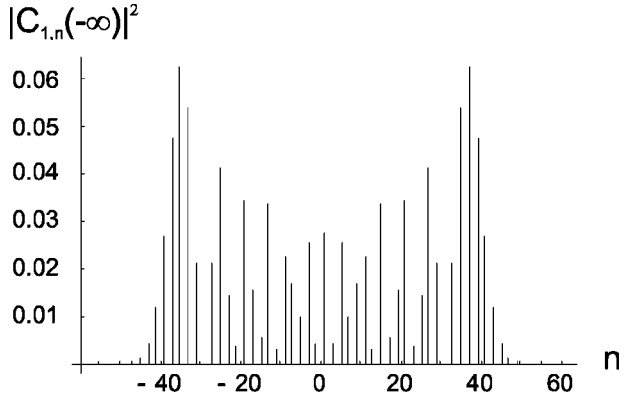

FIG. 3. Momentum distribution, generated by a far-off-resonant standing wave, which is used as the initial condition for a subsequent interaction with standing-wave laser pulses. The value $U=20$ is chosen for illustrative purposes and is in an intermediate range of experimentally accessible values.

γ (Fig. 2). As γ increases from zero, the oscillation amplitude as a function of α decreases monotonically; for values $\gamma\approx 1$ one finds that B no longer oscillates as a function of α. In the low intensity range ($0<\alpha\leqslant 1/2$) and for all intensities α for which $-1\leqslant B\leqslant 0$, the population transfer decreases with an increasing spontaneous emission rate. For all other field intensities, however, the transfer increases with increas-

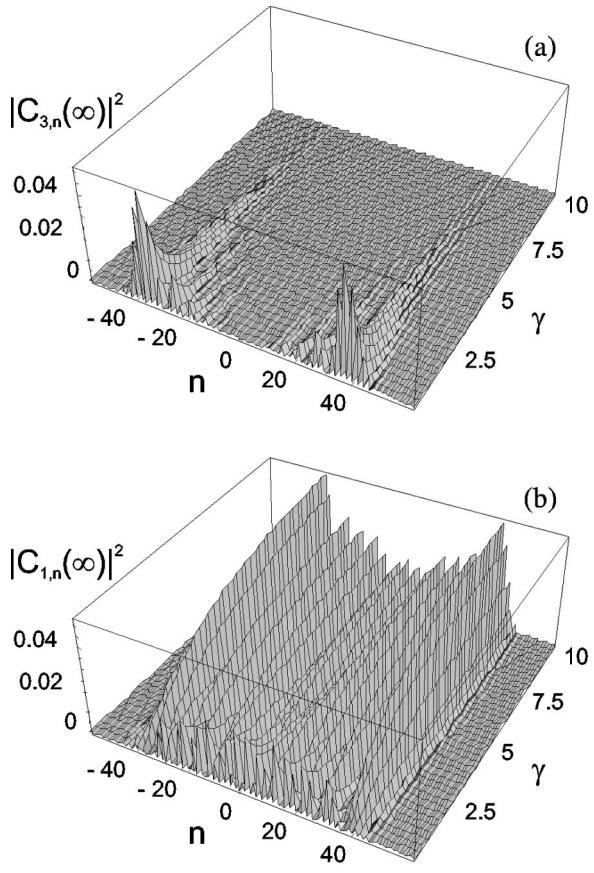

FIG. 4. Final momentum distribution for the initially populated (a) and initially empty (b) atomic internal energy levels for $\alpha=1$, $\beta=\delta=0$, and $\Omega_p(z)=\Omega\cos kz$, $\Omega_s(z)=\Omega\sin kz$.

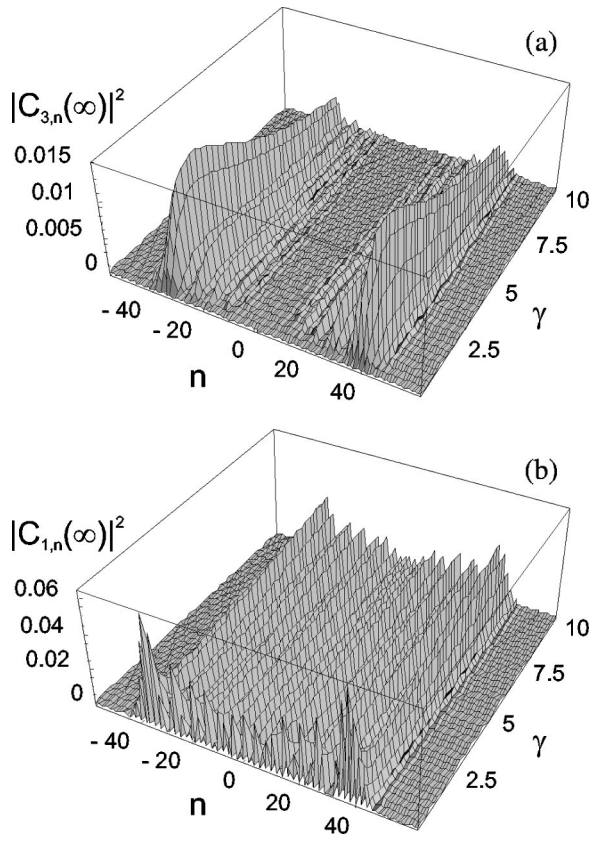

FIG. 5. Same as Fig. 4, except $\alpha=2$.

ing γ. In these regions of intensities, the completely coherent excitation would drive the atoms back to the initial state; spontaneous emission disturbs the coherent evolution and increases the population of state 3. Of course, when $\gamma \gg 1,\alpha,\beta,\delta$ (this region is not illustrated in Fig. 2), spontaneous decay severely limits the population transfer [the initial-state amplitude decays as $\exp(-\alpha^2/\gamma)$] and one finds $B \rightarrow 1$, $C_3(z,\infty)\rightarrow 0$, $C_1(z,\infty)\rightarrow C_1(z,-\infty)$. In these, as well as in all the other simulations, the initial-state amplitudes are given by Eq. (11); the initial-state populations are shown in Fig. 3.

The momentum distribution for each energy level as a function of γ is shown in Figs. 4 and 5. Figure 4 ($\alpha=1$) represents the case when coherent transfer into level 3 decreases for increasing γ (corresponding to π-pulse excitation). Figure 5 ($\alpha=2$) represents the contrary case when the increase of γ increases the coherent transfer into level 3 (corresponding to 2π-pulse excitation). Figures 4(b) and 5(b) illustrate the fact that there is no population transfer in the limit of very large γ.

We now examine the role of a chirp, $\beta\neq 0$, when $\gamma=\delta=0$. At $t=0$, the field is swept into resonance. Since Eq. (15) remains valid we need only consider the parameter

$$B(\alpha,\beta,0)=\frac{\cos(\pi\sqrt{\alpha^2-\beta^2})}{\cosh(\pi\beta)}. \tag{18}$$

This function is plotted in Fig. 6. For $\pi\beta>1$, one has B

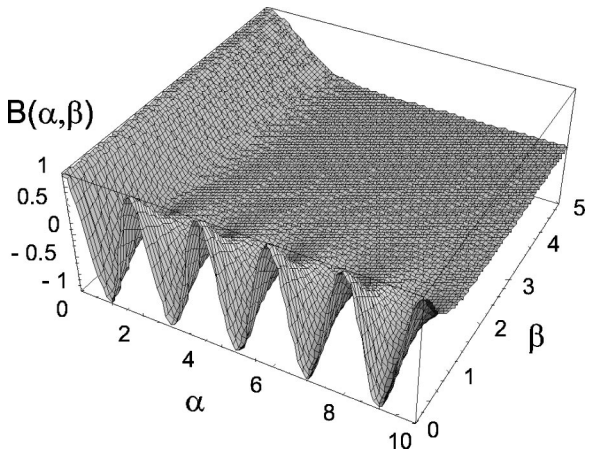

FIG. 6. Parameter B as a function of field intensity α and chirp parameter β for $\gamma=0$. Other parameters are the same as in Fig. 4.

≈ 0. Regardless of the other system parameters, the population transfer corresponds roughly to that achieved with a $\pi/2$ pulse.

B. cos-cos and sin-sin case

In this limit, when the standing-wave fields are in phase, it follows from Eq. (6) that θ is not z dependent, while the intensity parameter α is a trigonometric function of z. Since α appears in the arguments of the γ functions, this field geometry leads to a full Fourier spectrum and a rather complicated spectrum for the final-state population of state 3. There is a qualitatively different behavior of the various diffraction orders on γ than that of the sin-cos case. In Fig. 7 we present results analogous to those of Fig. 5(a) for the sin-sin case. As one sees, the damping in the central part of the momentum distribution is much more rapid than in the wings. This behavior provides an additional opportunity for suppressing intermediate momentum states, which are generated owing to nonexact $\pi/2$ shifts of the fields.

To illustrate the dependence of the results on the relative phase shifts of the fields, we show in Fig. 8 another plot analogous to Fig. 5(a), but for fields with phase shifts $\Delta\varphi$ averaged over the range $\pi/2-\pi/15\leqslant\Delta\varphi\leqslant\pi/2+\pi/15$. A

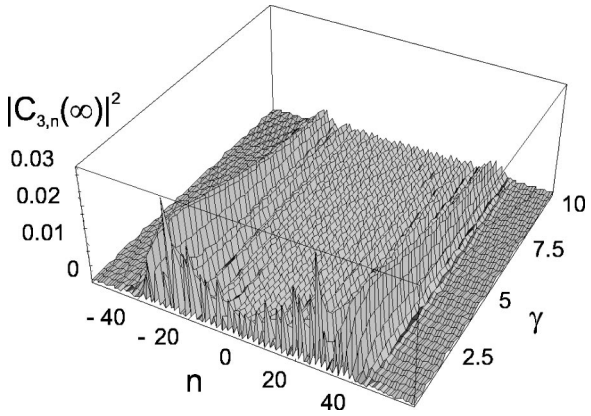

FIG. 7. Results analogous to those in Fig. 5(a), but for $\Omega_p(z)=\Omega\sin kz$, $\Omega_s(z)=\Omega\sin kz$.

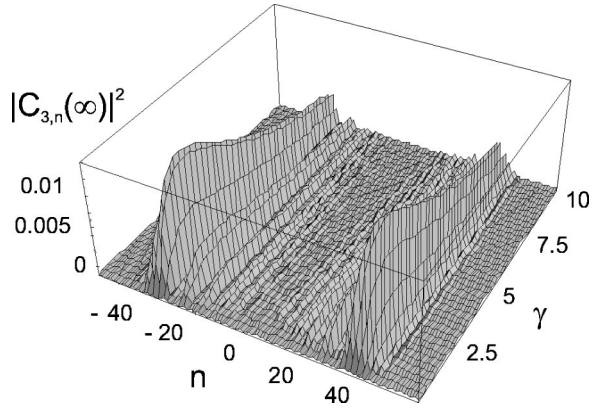

FIG. 8. Results analogous to those in Fig. 5(a) but averaged over a distribution of relative spatial phases between the fields, $\pi/2 - \pi/15 \leqslant \Delta\varphi \leqslant \pi/2 + \pi/15$.

comparison with the ideal results of Fig. 5(a) allows one to conclude that the operation of the phase-shifted beam splitter does not rely on the phase shift between the fields being precisely equal to $\pi/2$. For completeness, we note that the momentum distribution is asymmetric in general (see Fig. 9, drawn for a phase shift $\varphi=\pi/4$); only for phase shifts $\varphi=0$ and $\varphi=\pi/2$ is the momentum distribution symmetric. The asymmetry increases with increasing γ.

IV. ARBITRARY INITIAL STATE

Up to now the discussion was limited to an initial condition for which only level 1 is populated. In this section we examine the case where both lower-energy levels are populated, prepared using off-resonant standing-wave fields. In the case of $\pi/2$-shifted pulses [see formulas (12) and (13)] we arrive at

$$C_{3,n}(\infty)=\frac{B-1}{4i}[C_{1,n-1}(-\infty)-C_{1,n+1}(-\infty)] + \frac{B+1}{2}C_{3,n}(-\infty)+\frac{B-1}{4} \times[C_{3,n+1}(-\infty)+C_{3,n-1}(-\infty)], \tag{19}$$

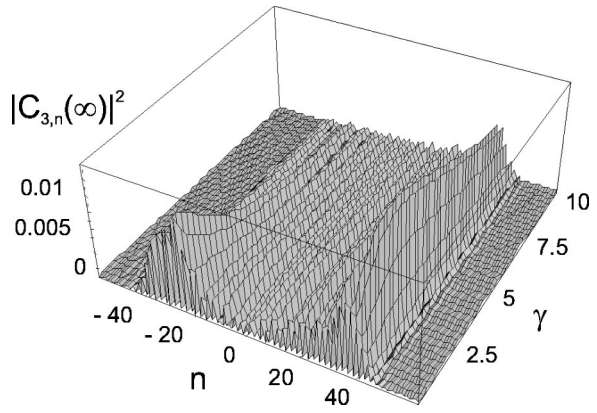

FIG. 9. Results analogous to those in Fig. 5(a) for a relative spatial phase $\varphi=\pi/4$. An asymmetry is present at $\gamma=0$ that increases with increasing γ.

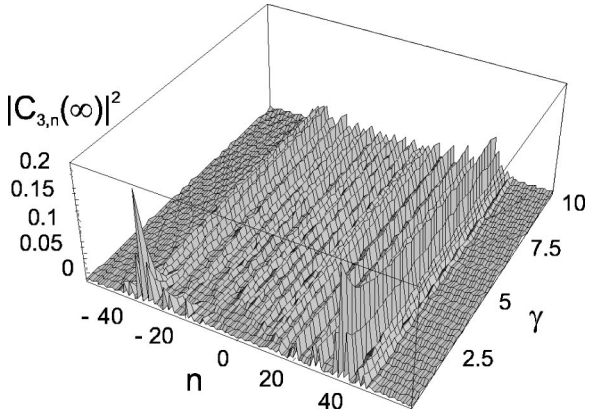

FIG. 10. Momentum distribution in level $|3\rangle$ in case when both levels were populated and prepared by means of far-off-resonant standing waves, shifted in space by $\pi/2$. $U=V=20$

the first term of which coincides with Eq. (14). We take an initial condition of the form

$$C_1(z,-\infty)=\frac{1}{\sqrt{2}}e^{iU\cos 2kz}=\frac{1}{\sqrt{2}}\sum_m i^m J_m(U)e^{2imkz}, \tag{20}$$

$$C_3(z,-\infty)=\frac{1}{\sqrt{2}}e^{iV\cos(2kz+\Phi)}=\frac{1}{\sqrt{2}}\sum_m i^m J_m(V)e^{im(2kz+\Phi)},$$

where V is the strength of the field driving the 2-3 transition and Φ is the relative phase of fields U and V. With this choice, one finds

$$\sqrt{2}C_{3,n}(\infty)=\frac{-B+1}{4}i^n[J_{n+1}(U)+J_{n-1}(U)] + \frac{B+1}{2}i^n e^{in\Phi}J_n(V)+\frac{B-1}{4}i^{n+1} \times e^{in\Phi}[e^{i\Phi}J_{n+1}(V)-e^{-i\Phi}J_{n-1}(V)]. \tag{21}$$

If one chooses $\Phi=\pi/2$, then suppression of intermediate momentum states occurs for both the first and third terms in this expression. The second term, which exhibits no such suppression, can be canceled only if $\gamma=0$ and $B=-1$. This possibility is illustrated in Fig. 10. The intermediate states can be canceled also for $\Phi=0$ by means of a special selection of parameters, but these results are not presented since they are of limited experimental use.

V. SUMMARY

In summary, we have shown that the interaction of a three-level atom with a pair of standing-wave laser pulses can lead to a large-angle atom beam splitter in a single internal atomic state. To produce a high quality beam splitter, it is necessary to prepare the initial state using one or more off-resonant standing-wave pulses. In this sense, the beam splitter geometry represents a type of compound lens, with

two atom-field interaction zones. Generalization to additional interaction zones is possible. The role of relaxation has been investigated by means of a scheme in which the relaxation takes place from the excited state to states outside the three-level system and the effects of frequency chirping have been considered. Relaxation can enhance or inhibit the transfer of population from initial to final state, depending on the field strength. Our proposed scheme possesses the principal advantages of beam splitters based on magneto-optical potentials or bichromatic fields, in that it leads to significant suppression of intermediate momentum components. The momentum state distributions of our beam splitter are similar to those achieved with magneto-optical or bichromatic field beam splitters, and clearly superior to that of standing-wave beam splitters. In contrast to magneto-optical or bichromatic field beam splitters which require specific values of the optical Rabi frequencies for most efficient operation, our beam splitter is fairly insensitive to the precise value of the Rabi frequency. More generally, it can be viewed as a type of building block for more complex atom beam splitters.

ACKNOWLEDGMENTS

This work was funded by Grant No. 0888 of Armenian Research Funds. The work of P.R.B. was supported by the U.S. Army Research Office under Grant No. DAAD19-00-1-0412 and the National Science Foundation under Grant No. PHY-0098016 and a FOCUS Center grant.

[1] *Atom Interferometry*, edited by P. R. Berman (Academic Press, Cambridge, 1997); C.S. Adams, O. Carnal, and J. Mlynek, Adv. At., Mol., Opt. Phys. **34**, 1 (1994).

[2] D.S. Weiss, B.C. Young, and S. Chu, Phys. Rev. Lett. **70**, 2706 (1993).

[3] P. Marte, P. Zoller, and J.L. Hall, Phys. Rev. A **44**, 4118 (1991); L.S. Goldner, C. Gerz, R.J.C. Spreeuw, S.L. Rolston, C.I. Westbrook, and W.D. Phillips, Phys. Rev. Lett. **72**, 997 (1994); P.D. Featonby, G.S. Summy, J.I. Martin, H. Wu, K.P. Zetie, C.J. Foot, and K. Burnett, Phys. Rev. A **53**, 373 (1996).

[4] J. Oreg, F.T. Hioe, and J.H. Eberly, Phys. Rev. A **29**, 690 (1984).

[5] A.M. Ishkhanyan, Phys. Rev. A **61**, 063609 (2000).

[6] P.R. Berman, B. Dubetsky, and J.L. Cohen, Phys. Rev. A **58**, 4801 (1998).

[7] K.S. Johnson, A. Chu, T.W. Lynn, K.K. Berggren, M.S. Shahriar, and M. Prentiss, Opt. Lett. **20**, 1310 (1995); M.K. Olsen, S. Choi, H.M. Wiseman, S.M. Tan, and D.F. Walls, Opt. Commun. **147**, 382 (1998); B. Dubetsky and P.R. Berman, Phys. Rev. A **64**, 063612 (2001).

[8] V.S. Voitsekhovich, M.V. Danileiko, A.M. Negriiko, V.I. Romanenko, and L.P. Yatsenko, Zh. Tekh. Fiz. **58**, 1174 (1988) [Sov. Phys. Tech. Phys. **33**, 690 (1988)]; Pis'ma Zh. Éksp. Teor. Fiz. **49**, 138 (1989) [JETP Lett. **49**, 161 (1989)]; R. Grimm, Yu.B. Ovchinnikov, A.I. Sidorov, and V.S. Letokhov, Phys. Rev. Lett. **65**, 1415 (1990); R. Grimm, J. Soding, and Yu.B. Ovchinnikov, Opt. Lett. **19**, 658 (1994); S.M. Tan and D.F. Walls, Opt. Commun. **118**, 412 (1995); T. Wong, M.K. Olsen, S.M. Tan, and D.F. Walls, Phys. Rev. A **52**, 2161 (1995); K.S. Johnson, A.P. Chu, K.K. Berggren, and M.G. Prentiss, Opt. Commun. **126**, 326 (1996); E.A. Korsunsky and Yu.B. Ovchinnikov, *ibid.* **143**, 219 (1997); A.S. Pazgalev and Yu.V. Rozhdestvenski, Pis'ma Zh. Eksp. Teor. Fiz. **66**, 412 (1997); J. Soding, R. Grimm, Yu.B. Ovchinnikov, P. Bouyer, and Ch. Salomon, Phys. Rev. Lett. **78**, 1420 (1997); E.A. Korsunsky, Quantum Semiclassic. Opt. **10**, 477 (1998); M. Williams, F. Chi, M. Cashen, and H. Metcalf, Phys. Rev. A **61**, 023408 (2000); V.I. Romanenko, and L.P. Yatsenko, Zh. Éksp. Teor. Fiz. **117**, 467 (2000) [JETP Lett. **90**, 407 (2000)].

[9] R. Grimm, V.S. Letokhov, Yu.B. Ovchinnikov, and A.I. Sidorov, J. Phys. II **2**, 593 (1992); T. Pfau, Ch. Kurtsiefer, C.S. Adams, M. Sigel, and J. Mlynek, Phys. Rev. Lett. **71**, 3427 (1993); C.S. Adams, T. Pfau, Ch. Kurtsiefer, and J. Mlynek, Phys. Rev. A **48**, 2108 (1993); C.S. Adams, T. Pfau, and J. Mlynek, in *Atomic Physics 13*, edited by H. Walther, T. W. Hänsch, and B. Neizert, AIP Conf. Proc. No. 275 (AIP, New York, 1993), p. 200; U. Janicke and M. Wilkens, Phys. Rev. A **50**, 3265 (1994); J. Soding and R. Grimm, *ibid.* **50**, 2517 (1994); A.P. Chu, K.S. Johnson, and M.G. Prentiss, J. Opt. Soc. Am. B **13**, 1352 (1996).

[10] V.M. Arutunyan and A.Zh. Muradyan, Dokl. Akad. Nauk Arm. SSR **60**, 275 (1975); R.J. Cook and A.F. Bernhardt, Phys. Rev. A **18**, 2533 (1978); A.P. Kazantsev, G.I. Surdutovich, and V.P. Yakovlev, Pis'ma Zh. Éksp. Teor. Fiz. **31**, 542 (1980) [JETP Lett. **31**, 509 (1980)]; J. Dalibard and C. Cohen-Tannoudji, J. Opt. Soc. Am. B **2**, 1707 (1985); P. Meystre, E. Schumacher, and S. Stenholm, Opt. Commun. **73**, 443 (1989); P.J. Martin, P.L. Gould, B.G. Oldaker, A.H. Miklich, and D.E. Pritchard, Phys. Rev. A **36**, 2495 (1987).

[11] J.L. Cohen, B. Dubetsky, and P.R. Berman, Phys. Rev. A **61**, 033610 (2000).

[12] C.E. Carroll and F.T. Hioe, J. Math. Phys. **29**, 487 (1988); N.V. Vitanov, J. Phys. B **31**, 709 (1998).

[13] A.S. Pazgalev and Yu.V. Rozhdestvenski, Zh. Eksp. Teor. Fiz. **109**, 2005 (1996).

[14] See, for example, in *Handbook of Mathematical Functions*, edited by M. Abramowitz and I. A. Stegun (Dover, New York 1972), p. 364.